Dose Estimation in Strontium-89 Radiotherapy of Metastatic Prostatic Carcinoma

Stephen L. Breen,* J. E. Powe,† and A. T. Porter

Departments of Medical Biophysics, Diagnostic Radiology & Nuclear Medicine, and Oncology, University of Western Ontario; Department of Nuclear Medicine, Victoria Hospital and London Regional Cancer Centre, London, Ontario, Canada

Strontium-89 radiotherapy is becoming an important treatment in the palliation of bone pain from osteoblastic metastases. The absorbed dose delivered to bone metastases during ^{89}Sr radiotherapy has been estimated in four patients with metastatic prostatic carcinoma. Patients were injected with a tracer dose of ^{85}Sr-chloride. Blood and urine samples were obtained during the week following injection. Strontium-85 scintigrams of metastases and normal bone were obtained up to 8 wk postinjection. Half of the patients showed elevated whole-body retention; plasma-strontium concentrations were decreased from normal values. Uptake of strontium in metastases was 2–25 times that in normal bone but rates of washout of strontium from metastases were similar to those from normal bone. Absorbed doses delivered in infinite time to the metastases by ^{89}Sr ranged from 21 ± 4 to 231 ± 56 cGy/MBq with a median value of 68 cGy/MBq. Doses to red marrow were less by a factor of 2 to 50. These absorbed doses are sufficiently large to be expected to produce a therapeutic benefit.

J Nucl Med 1992; 33:1316–1323

The use of ^{89}Sr in the palliation of pain from metastasized prostatic carcinoma was first reported by Pecher (*1*) in 1942. Indeed, strontium was the first radionuclide used in the palliation of bone pain from osseous metastases. In a more rigorous study in 1950, Lawrence (*2*) showed that ^{89}Sr and ^{32}P controlled pain in a group of patients with metastatic bone disease. Phosphorus-32 is effective in inducing palliation in 50%–70% of patients, but it is associated with a high degree (>30%) of hematological toxicity (*3*). Because strontium is not involved to the same extent as phosphorus in metabolic pathways, hematological toxicity is less.

In the last 15 yr, the effectiveness of strontium radiotherapy has been demonstrated by a number of authors (*4–7*). Typically, 20% of patients become pain free and a further 60% show some relief of pain. However, only a few investigators have attempted to estimate the absorbed dose delivered to metastases. Their results are summarized in Table 1.

In order to calculate the absorbed dose to the lesions, Firusian (*8*) made several assumptions about the biodistribution of strontium. By assuming that two-thirds of the injected activity will be stored in the skeletal system and that the skeleton accounts for 10% of the body weight, a dose of 0.555 kBq of ^{89}Sr per kg body weight will give an activity concentration of 3.7 kBq per kg skeletal weight. If the metastases concentrate activity at five times the rate of normal bone, the activity concentration in the metastases should be 18.5 kBq per kg. There were no significant changes in red blood cell and leukocyte counts.

Silberstein and Williams (*9*) treated 38 patients with osseous metastatic disease. A dosimetry schema (for occupationally exposed workers) developed by the International Commission on Radiological Protection (ICRP) was used to estimate absorbed doses to red marrow and to metastases by assuming that the metastases would incorporate strontium at five times the rate of normal bone. Of the 45 treatments, 22 showed no response and 23 showed some improvement. The median response time was nine days; responses lasted an average of 1.6 mo. No hematological toxicity was observed.

Tennvall et al. (*4*) treated eleven patients under two treatment plans: eight patients received three injections of 100 MBq of ^{89}Sr at 4-wk intervals; three patients received one 200 MBq injection. Strontium-89 uptake was estimated by obtaining bremsstrahlung scintigrams at four weeks. Five of the patients in the first group responded to the therapy; none of the second group responded. Only in cases involving substantial marrow involvement was hematological toxicity observed.

Blake has investigated several aspects of strontium therapy, including strontium kinetics (*10,11*) and absorbed dose estimation (*12,13*). The Medical Internal Radiation Dosimetry (MIRD) formalism (*14*) was used to estimate the absorbed dose to metastases. Strontium localization in metastases was observed by obtaining ^{85}Sr scintigrams of lesions.

We have investigated the localization of strontium in

Received Oct. 25, 1991; revision accepted Mar. 10, 1992.

For reprints contact: Stephen L. Breen, MSc, Physics Department, London Regional Cancer Centre, 790 Comissioners Rd. E., London, Ontario, Canada N6A 4L6.

Current Addresses: * Physics Department, London Regional Cancer Centre, London, Ontario, Canada.

† Department of Radiation Oncology, Wayne State University and Harper Hospital, Detroit, Michigan.

TABLE 1
Summary of Previous ^{89}Sr Dosimetry Studies

Author	Method of dose estimation	Activity administered	Dose to lesion	Dose to red marrow
Firusian (*8*)	ICRP model	74 MBq	110 cGy in 8 days	—
Silberstein and Williams (*9*)	ICRP model	3.7 MBq/kg	8.1 cGy/MBq in 2 yr	1.0 cGy/MBq
Tennvall et al. (*4*)	ICRP model	300 MBq 200 MBq	45 Gy/yr 30 Gy/yr	1 cGy/MBq
Blake et al. (*12,13*)	Imaging and MIRD	99–240 MBq	3–138 Gy over infinite time	1 cGy/MBq

All authors used the ICRP model of strontium dosimetry to estimate the absorbed dose to red marrow.

the skeletons of four patients, all with metastasized prostatic carcinoma. In addition, the whole-body retentions, plasma-strontium concentrations and renal plasma clearance rates were measured in five patients. Estimates of the absorbed dose delivered to metastases in the spine, pelvis and long bones were made in four patients.

METHODS

Five males, all with metastasized prostatic carcinoma, had had ^{99m}Tc-methylene diphosphonate bone scans. From the scans, the extent of metastatic disease in the patients was determined and lesions were selected for dosimetric study. After the technetium bone scans, the patients were injected with 37 MBq of ^{85}Sr-chloride. Anterior and posterior images of the lesions were obtained using a Searle LFOV scintillation camera equipped with a high-energy collimator. Images were recorded for 15 min at each site at 4 hr, 2 days, and 1, 2, 4 and 8 wk following the injection. During the week following injection, blood samples and urine samples were collected. Patients received a therapeutic injection of 150 MBq of ^{89}Sr within 7 days of the ^{85}Sr injection. The physical properties of both these radionuclides are given in Table 2.

Whole-body Strontium Kinetics

In order to estimate the whole-body retention of strontium, urine was collected in 12-hr pools for the first 4 days after injection and then in 24-hr periods for another 2 days. Samples were counted in duplicate 1-ml aliquots in a multichannel analyzer (Searle model 1185) whose sensitivity was measured with a ^{85}Sr source. It was assumed that fecal clearance was insignificant, as studies have shown (*12*) that most patients, including our own, complained of constipation, usually related to narcotic use for pain relief.

TABLE 2
Physical Properties of ^{85}Sr and ^{89}Sr

	^{85}Sr	^{89}Sr
Transition	Electron capture	β^-
Emission energy	E_γ = 514 keV	E_{max} = 1.46 MeV
Half-life	64.8 days	52 days
Mean number per disintegration	>0.99	>0.99

The ICRP has developed a model for the metabolism of alkaline earth elements (*15*). We compared the whole-body retention of our subjects with the model developed by the ICRP. Neglecting terms relating to long-lived ($t_{1/2} > 10^3$ days) compartments, the ICRP model for strontium retention can be simplified to

$$R(t) = (1 - f)e^{-mt} + f\left(1 + \frac{t}{\epsilon}\right)^{-b} \qquad \text{Eq. 1}$$

where

$R(t)$ = whole-body retention;
f = fraction of strontium not in short-lived pool; = 0.60;
m = rate constant corresponding to a short-lived compartment
= 0.25/day;
ϵ = a small time relating to a delay in uptake
= 0.20 day;
b = slope of power-law retention term
= 0.18.

The plasma-strontium concentration, $P(t)$, was measured by drawing blood samples from the patients at 5, 15, 30 and 60 min postinjection, and at 2, 4 and 8 hr, and then daily up to 7 days. Samples were centrifuged to separate the plasma, which was then counted in duplicate 1-ml samples. The ICRP model can be used to calculate the plasma-strontium concentration, since

$$P(t) = \frac{1}{k}\left|\frac{dR}{dt}\right|, \qquad \text{Eq. 2}$$

where k is the endogenous plasma clearance rate. The plasma concentration is then given by

$$P(t) = \frac{1}{k}\left[m(1 - f)e^{-mt} + \frac{fb}{\epsilon}\left(1 + \frac{t}{\epsilon}\right)^{-(b+1)}\right]. \qquad \text{Eq. 3}$$

Renal plasma clearance rates of strontium were also calculated. The renal plasma clearance rate is given by

$$k_{renal} = \frac{\int_{t_1}^{t_2} dU}{\int_{t_1}^{t_2} P(t)dt}, \qquad \text{Eq. 4}$$

where dU = the fraction of the injected dose of strontium excreted by the kidneys in time dt. The numerator of this expression is the amount of strontium excreted through the kidneys during the period t_1 to t_2. The denominator is the integral of the plasma time-activity curve over the same interval. A linear regression analysis was performed on these data to determine the renal plasma clearance rate of strontium. All of the curves were forced through the origin. The normal value of k_{renal}, according to the ICRP model for strontium metabolism, is 8.3 liters/day.

Absorbed Dose Estimates

Absorbed doses were calculated with the MIRD formalism. The absorbed dose is given by

$$\bar{D} = 1.385 \times 10^{-2} \tilde{A} \Delta \frac{\phi}{m_t}, \qquad \text{Eq. 5}$$

where

$\bar{D}$ = the average absorbed dose (Gy);
$\tilde{A}$ = cumulated activity (MBq-days);
Δ = mean energy (keV);
ϕ = absorbed fraction (dimensionless);
m_t = mass of target tissue (g).

The mean energy of the beta emissions of ^{89}Sr is 583 keV. Because of the short range of the beta particles, the absorbed fraction in the metastases can be taken to be one. The mass of the target tissue, m_t, was estimated by assuming a density of 1.5 g/cm^3 (as found by Blake et al. (*13*) using quantitative CT techniques) and estimating lesion volumes from MR, x-ray and scintigraphic images. In vertebral bodies, the volume of the lesion was determined by estimating, from the technetium bone scans, the fraction of the lesion that was metabolically active. The cumulated activity, $\tilde{A}$, is the number of nuclear decays that occur in a given time interval, and is therefore the area under a time-activity curve.

Several investigators have used the conjugate view technique to determine the amount of activity in a region of interest (*16–18*). The conjugate view technique requires opposing views of the source of activity and an estimate of the size of the lesion and the patient thickness. The activity can be calculated with the expression

$$A = \sqrt{\frac{C_A C_P}{e^{-\mu_e d}}} \frac{1}{E} \frac{\mu_s s/2}{\sinh(\mu_s s/2)}, \qquad \text{Eq. 6}$$

where

A = activity in the region of interest (MBq);
C_A = count rate in the anterior view (cps);
C_P = count rate in the posterior view (cps);
d = patient thickness (cm);
μ_e = effective attenuation coefficient across the patient thickness (cm^{-1});
E = camera sensitivity (cps/MBq);
s = thickness of region containing activity (cm);
μ_s = attenuation coefficient of region containing activity (cm^{-1}).

The last factor in Equation 6 is the volume correction term. This correction term is small over all reasonable source sizes and can therefore be neglected. Equation 6 then becomes

$$A = \sqrt{\frac{C_A C_P}{e^{-\mu_e d}}} \frac{1}{E}. \qquad \text{Eq. 7}$$

The error in this method is due to the uncertainty in the thickness and shape of the source and the activity distribution in it. The exponential term in Equation 7 accounts for attenuation by the patient. This can be measured with a transmission view. However, a transmission view for strontium would require a very hot source in order to accomplish the imaging in a reasonable amount of time. This would give a high dose to the technologist, and the source would require a large amount of lead shielding during storage. Instead, the soft-tissue attenuation coefficient was approximated with the attenuation coefficient measured in a water phantom. This was used, along with a tabulated value for the attenuation coefficient of bone, to determine an effective attenuation factor. Patients' thicknesses and lesion dimensions were measured from MR or x-ray images.

Strontium-85 scintigraphic images of a given lesion were aligned by cross-correlating the x- and y- projections of the images. An irregular region of interest (IROI) was drawn around the lesion, and this was superimposed on all the images of a given lesion to obtain the anterior and posterior count rates C_A and C_P.

The absorbed dose delivered to red marrow was calculated in a similar manner. Vertebral bodies that showed the lowest degree of involvement were selected. Half of the counts in this ROI were assumed to originate in trabecular bone, as described by the ICRP model for strontium metabolism (*15*). The ICRP model for bone dosimetry (*19*) gives an absorbed fraction of 0.42 for ^{89}Sr beta particles from trabecular bone to red marrow.

RESULTS

Five patients took part in the kinetics portion of this study; one was not able to take part in the imaging and dose estimation part of the study. The disease states of all of the patients are described in Table 3.

Strontium Kinetics

Plots of whole-body strontium retention are shown in Figure 1. Three of the five patients showed strontium retentions in excess of the values predicted by the ICRP model. Moreover, the retentions correlate positively with the extent of the patients' metastatic disease as described in Table 3. In two of the patients' (WP and RH) scintigraphic images, some strontium was seen in the gut, so the assumption of negligible fecal clearance may be not be totally appropriate. Regardless, the increased retention of the strontium is quite significant, especially in Patient AM.

TABLE 3
Extent of Metastatic Disease in Subjects

Patient	Extent of metastatic disease
WP	Limited metastatic disease. Eight sites including extensive pelvis involvement.
WK	Multiple metastatic lesions in ribs and pelvis. Moderately extensive disease in spine.
RH	Extensive spine and pelvis involvement with more marked intensity than WK.
AM	"Superscan," showing metastatic involvement in essentially every bone.
OS	Multiple discrete and intense metastases (greater than 100 sites).

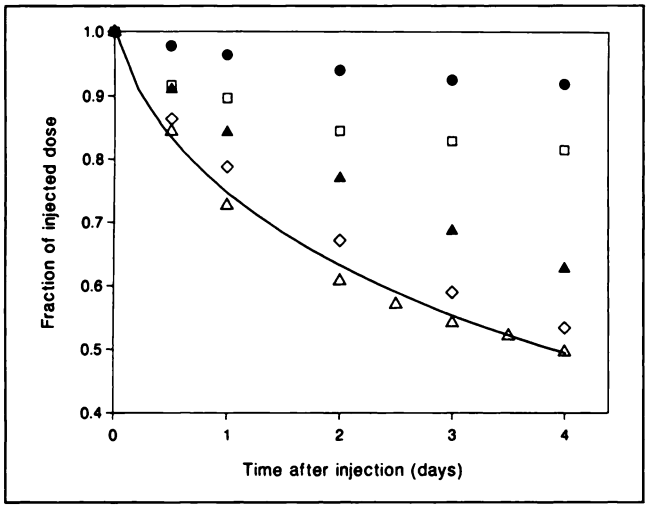

FIGURE 1. Whole-body strontium retention up to 4 days after injection. WK-▲; WP-△; AM-●; OS-□; RH-◇. Solid line is ICRP model.

Plasma-strontium concentrations up to 7 days postinjection are shown for all patients in Figure 2. Two patients showed plasma concentrations that were much less than would be expected from the ICRP model. These same two patients who showed the lowest plasma concentrations also showed the highest degree of strontium retention.

Renal plasma clearance rates for strontium were calculated by plotting the integrated renal excretion against the time integral of the plasma-strontium concentration as in Equation 4. These plots show a large degree of scatter (Fig. 3), due likely to the difficulty of obtaining timed urine collections (e.g., patients not completely emptying their bladder at the end of each time interval), especially in this group of patients with prostate disease. The renal plasma clearance rates are tabulated in Table 4. All values are

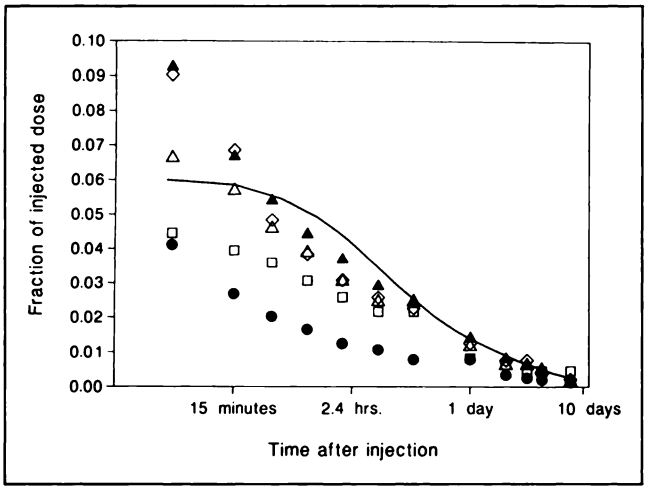

FIGURE 2. Plasma-strontium concentration up to 7 days post-injection. WK-▲; WP-△; AM-●; OS-□; RH-◇. Solid line is ICRP model.

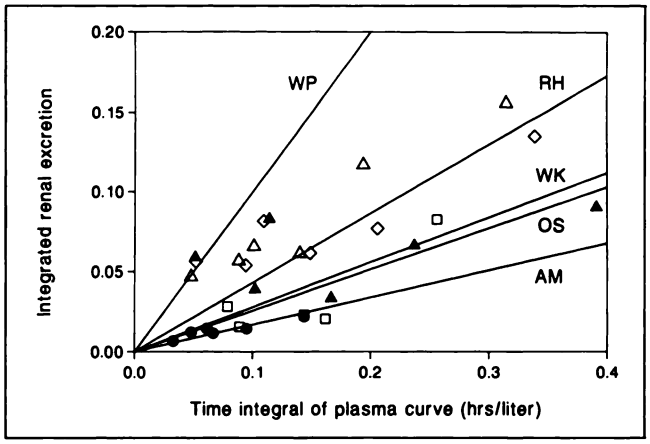

FIGURE 3. Renal plasma clearance rates of strontium. WK-▲; WP-△; AM-●; OS-□; RH-◇.

within the normal range with the exception of Patient AM. This patient has the most extensive metastatic disease.

Strontium-85 Imaging

The use of a high-energy gamma-emitting isotope like ^{85}Sr ($E_{photopeak}$ = 514 keV) results in images of relatively poor quality for a number of reasons. The sensitivity of the camera is very low (about 200 cpm/MBq) because of the low geometric efficiency of the high-energy collimator and because of the low sensitivity of the NaI(Tl) crystal at this energy. The spatial resolution of the camera is also worsened because of the high-energy collimator. These shortcomings of the strontium images are apparent in the scintigrams shown in Figure 4.

The poor spatial resolution of the camera prevented the precise localization of the activity in regions where the lesions were closely spaced. In such cases, the activity must be quantified by using a single region of interest imposed on several lesions. The absorbed dose calculated will be the average absorbed dose delivered to these lesions.

Variations in camera sensitivity were investigated using a strontium source in a water phantom. This simulates patient imaging more closely than a measurement of sensitivity in air. Twenty measurements over the course of several months showed that the sensitivity averaged 218 ± 31 cps/MBq. This large variation in sensitivity was thought to be due to drift in the acceptance window of the camera.

TABLE 4
Clearance Rates of Strontium from Renal Plasma

Patient	Renal plasma clearance rate ± σ (liters/day)
Normal	8.3 ± 3
WK	6.7 ± 2.6
AM	4.1 ± 0.8
OS	6.2 ± 2.4
WP	12.8 ± 1.7
RH	10.4 ± 2.5

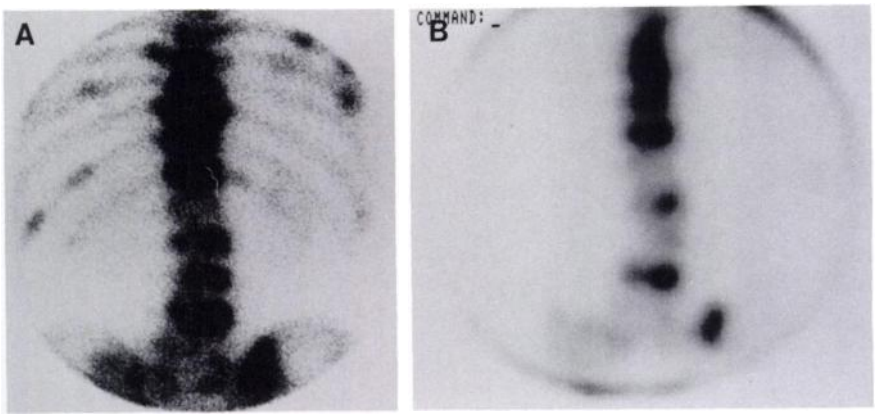

FIGURE 4. Posterior spine views of Patient RH. (A) ^{99m}Tc-MDP scan. (B) ^{85}Sr bone scan.

The sensitivity drifted slowly, so any changes during imaging sessions were negligible. When possible, the sensitivity was measured using a strontium source in a soft-tissue phantom before each imaging session.

Localization and Retention of Activity

The conjugate view technique described previously was used to quantitate the activity in lesions and in normal bone. Three of the four patients were followed for 28 days, while a fourth was followed for 56 days. The strontium in metastases and normal bone, as a percent of the injected dose per kilogram of the material containing the activity, is plotted against time for two patients in Figure 5. The area under these curves is proportional to the cumulated activity, $\tilde{A}$. The large standard deviation of the individual data points (calculated, using standard error propagation techniques (*20*), from the uncertainties in each term of Equation 7) is a result of uncertainty in the depth of the source of activity and in the camera sensitivity, and also as a result of poor statistics.

The data in Figure 5A are from a patient with several isolated metastases. These sites show a decrease in the activity over time. The data in Figure 5B are from a patient with metastatic involvement in almost every bone. In this case, there was no removal of the strontium from any site. In general, there are variations in the degree of strontium uptake and in its rate of removal from lesions from patient to patient, and from lesion to lesion in a given patient. In all patients, the strontium concentration in metastatic lesions was from 2 to 25 times greater than in normal bone.

The data of Figure 5 show the retention of ^{85}Sr after correction for physical decay. These retention data were fitted with a monoexponential decay to estimate the biological half-life of the strontium; these results are shown in Table 5. Longer half-times will result in greater absorbed doses. Biological half-times in lesions did not appear to be different from those in normal bone.

Strontium-89 Dose Estimation

Strontium-89 doses were estimated for the period over which strontium images were obtained. The dose over this period was calculated by correcting the data for the retention of ^{85}Sr for its physical decay and for the decay of ^{89}Sr. A trapezoidal integration of the resulting time-activity curves was performed to find the cumulated activity, $\tilde{A}$, of ^{89}Sr. This result was placed in Equation 5 to get the absorbed dose.

The dose over an infinite time was estimated by fitting the retention data with a monoexponential decay in order to determine the biological half-time (see Table 5). Estimates of the dose delivered after 28 days and the dose delivered over an infinite time are shown in Table 6. The absorbed doses over infinite time range from 21 ± 4 to 231 ± 56 cGy/MBq, with a median value of 68 cGy/MBq.

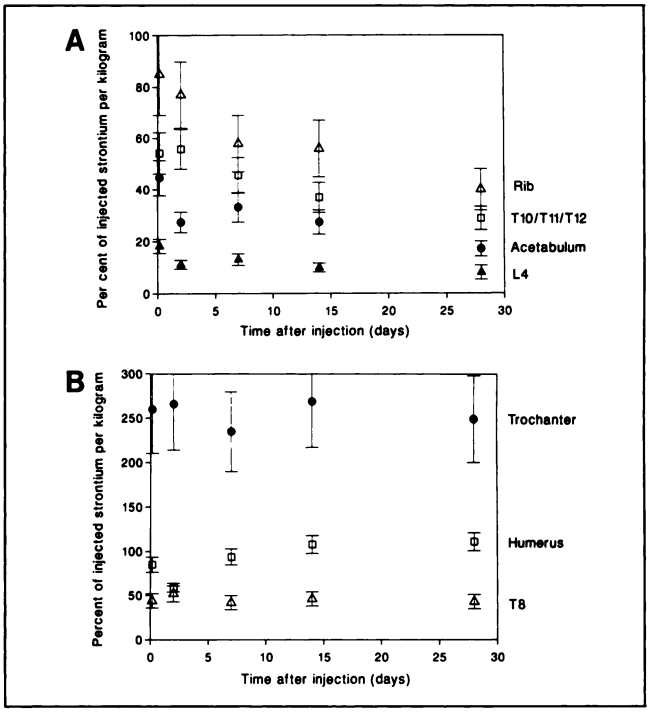

FIGURE 5. Strontium retention in two patients as a fraction of injected dose per kilogram of activity-containing material. (A) For WK, L4 is normal bone; (B) for AM, T8 is normal bone.

TABLE 5
Biological Halftimes for Strontium Retention in Metastases

Patient	Site	Biological half-time ± σ (days)
WK	T10/T11/T12	27 ± 3
	Acetabulum	20 ± 1
	Rib	24 ± 5
	L4*	20 ± 4
AM	Humerus	—
	Trochanter	—
	T8*	137 ± 27
WP	L1	56 ± 28
	T8	53 ± 12
	T12*	41 ± 8
RH	L4	—
	Trochanter	—
	T10/T11/T12	104 ± 14
	L2/L3	—
	SI joint	63 ± 19
	Acetabulum	—
	L1*	46 ± 13

Where no value is given, there is complete retention of the strontium.
* Normal bone.

DISCUSSION

Strontium Kinetics

The ^{85}Sr scintigrams showed increased uptake of strontium in the metastases of all patients. The pattern of uptake in the scintigrams was very similar to that seen on the ^{99m}Tc-methylene diphosphonate scintigrams. The time-activity curves of Figure 5 show that strontium is concentrated in the lesions to a much higher level than in normal bone. This agrees with the measurements of whole-body strontium kinetics. The biological half-times of strontium in the skeleton are much greater than the 2-wk half-time predicted for normal subjects. It is this combination of a high degree of localization and a long period of retention that causes the high doses to lesions and the high tumor-to-red marrow dose ratio.

The whole-body retention curves show that strontium retention correlates positively with the extent of metastatic disease. In addition, the lower-than-normal plasma concentrations of the strontium indicate that, while the strontium is being retained to a greater extent than would be expected in a normal subject, it is not being retained in plasma.

Figure 5 shows time-activity curves for selected lesions and for normal bone for two patients. There was no correlation between the degree of retention of the strontium in lesions and the extent of disease in the patients. In addition, there is no clear relationship between the whole-body retention of plasma and the degree of retention of the strontium in lesion sites. Blake et al. (*11*) have shown the importance of renal plasma clearance rates on strontium retention. However, the retention in individual lesion sites appears to be independent of renal plasma clearance. In patients with decreased renal clearance, the strontium will be excreted at a slower rate, and there will be more time for it to be absorbed in lesion sites. The ability of the individual metastases to take up and retain strontium appears to be a greater factor in determining the absorbed dose delivered to the metastases.

Models for strontium retention give biological half-times in the skeleton on the order of 2 wk. Table 5 shows much greater half-times in all patients, in both normal bone and in lesions. There was no apparent difference in the residence time between normal bone and metastatic sites. This may be due to the presence of metastatic tissue in bone that was thought to be without lesions, especially in patients with extensive disease. In addition, scatter from regions of high activity may contribute to the activity attributed to normal bone.

The whole-body kinetics of strontium in this group of patients is quantitatively similar to the results of Blake et al. (*10*), who showed variations in the uptake and retention of strontium from patient to patient. However, we have found additional variations in strontium uptake and retention from lesion to lesion in each patient.

TABLE 6
Estimates of Absorbed Doses from ^{89}Sr to Metastases and Normal Tissue

Patient	Site	Dose Estimate ± σ (cGy/MBq) After 28 days	Dose Estimate ± σ (cGy/MBq) After infinite time
WK	T10/T11/T12	7.7 ± 1.6	21 ± 4
	Acetabulum	5.2 ± 1.4	35 ± 11
	Rib	10.7 ± 2.6	48 ± 24
	Red marrow	1.7 ± 0.3	7 ± 5
AM	Humerus	18.2 ± 3.9	59 ± 5
	Trochanter	42 ± 10.0	137 ± 10
	Red marrow	8.5 ± 0.8	19 ± 3
WP	L1	2.5 ± 0.6	231 ± 56
	T8	7.8 ± 1.7	68 ± 33
	Red marrow	0.6 ± 0.1	4.5 ± 2.2
RH	L4	19.4 ± 4.1	62 ± 5
	Trochanter	42 ± 10.0	135 ± 20
	T10/T11/T12	17.3 ± 3.6	148 ± 32
	L2/L3	21.9 ± 4.6	71 ± 8
	SI joint	33.2 ± 7.5	213 ± 155
	Acetabulum	20.9 ± 4.4	67 ± 6
	Red marrow	5.9 ± 2.0	33 ± 21

Red marrow dose estimates are based on measurements from normal vertebrae.

Absorbed Dose Estimates

Absorbed dose estimates for metastatic lesions and for red marrow in all patients are shown in Table 6. Typical treatments at our institution consist of an injected dose of 150 MBq of ^{89}Sr, so an absorbed dose of 20 cGy/MBq

would result in a total dose of 3000 cGy, which is thought to be large enough to produce a therapeutic effect. In our study, estimates of the dose delivered to lesions over infinite time for 150-MBq injections of ^{89}Sr ranged from 3000 ± 600 to 30,000 ± 10,000 cGy. These results concur with those of other investigators (*4,8,9,12,13*) who have estimated absorbed doses. However, it is difficult to make direct comparisons of the results because the doses are given for different periods of time. The increased uptake of strontium by metastases was correctly predicted, and the estimates of the absorbed doses of all the investigators are in agreement. Differences may be largely due to the methods of estimation and the extent of disease of the patients.

A limiting factor in these dose estimates was the poor resolution of the strontium images (Fig. 4B) because of the high-energy collimator. Although the low sensitivity of the camera caused relatively poor counting statistics, uncertainties in the position of the source of activity and uncertainties in the camera sensitivity were the greatest sources of error in the quantitation of activity.

The confounding factor of dose rate has to be taken into account when comparing doses achieved with strontium therapy to those achieved with external beam radiotherapy. It is well recognized that the low dose rate seen in brachytherapeutic applications (i.e., less than 100 cGy/hr) is a major factor in reducing the biological effect of a given dose. This is due to two major factors: the repair of sublethal damage and effect of proliferation.

An analogy can be drawn from the clinical literature (*21*) in which doses of 6000–7000 cGy are found to be highly effective in the sterilization of small volume ($B_{1/2}$) prostate cancer, but in using a permanent iodine implant (^{125}I has a physical half-life of 60 days) and similar dose rates, as occurs with ^{89}Sr therapy, doses in the range of 16,000 to 24,000 cGy are required.

Kirk et al. (*22*) have developed a model relating the absorbed dose and the half-time of irradiation for brachytherapeutic applications. This sort of analysis can be applied to strontium radiotherapy to account for the dose rate effect. A curve of constant radiobiological effect for different combinations of absorbed doses and effective half-lives (corresponding to a typical treatment (*23*) of 24 Gy in six daily fractions of external beam radiotherapy) is shown in Figure 6. Superimposed on this curve are the data for all the metastases studied in this investigation. The isoeffect line provides only an approximation since it is based upon radiobiological data for sublethal damage to normal tissue; the dose rate effect in strontium radiotherapy will depend upon lethal damage to neoplastic tissue. However, this curve gives a rough idea of the combinations of absorbed doses and half-lives that will produce a radiation effect equivalent to an external beam treatment. It can be seen that most of the data points lie above the isoeffect line.

The dose estimates for red marrow are, in most cases,

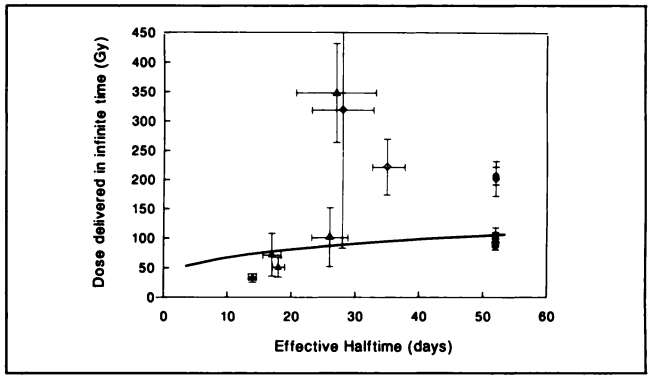

FIGURE 6. Isoeffect curve demonstrating the dose rate effect. The solid line corresponds to an effect equivalent to a typical external beam radiotherapy treatment. Data points are for doses delivered by ^{89}Sr over infinite time to lesions in each patient. WK–▲; WP–△; AM–●; RH–◇.

much less than the doses delivered to metastatic lesions. However, in absolute terms, they are somewhat high, ranging from 675 to 5000 cGy for injections of 150 MBq of ^{89}Sr. This may partially be due to counts originating in metastatic lesions that were included in IROIs drawn around normal bone. One patient (AM) who had extensive metastatic disease may have had metastatic disease in all vertebral bodies with little red marrow remaining in the vertebral bodies, so these dose estimates may not be accurate. Finally, the doses are delivered over a long interval, and as a result the dose rate effect will lessen the radiobiological damage. As mentioned previously, other investigators suggest bone marrow doses on the order of 1 cGy/MBq; the true value may lie between this value and the values found in this work. The subject of hematological toxicity has been studied by Cowan (*24*), who describes the potential for red marrow toxicity during ^{89}Sr radiotherapy.

The major shortcoming of this macroscopic dose estimate is that it ignores two important factors. First, the metastatic lesion is composed of a mixture of neoplastic cells and bone mineral. These two materials have different radiological properties because of their different densities and atomic composition. As a result, the distribution of the absorbed dose in this inhomogeneous material is not known. The second complication is that the distribution of the strontium in the lesion is also unknown. Because the beta particles have a short range (about 2 mm in bone and 7 mm in soft tissue), only the cells close to regions containing strontium will be irradiated. The amount of strontium present in a given region of a metastasis will depend on the rate of bone remodeling and the vascular supply to the region. Thus, there will be further inhomogeneities in the dose distribution in a lesion because of the nonuniform distribution of the radionuclide. We intend to address these issues in our further investigations of strontium radiotherapy. Additionally, we hope to answer more completely the questions regarding the dose rate

effect. The results of these investigations will be of use in many types of unsealed source radiotherapy.

CONCLUSIONS

All the patients involved in this study showed increased whole-body retention of strontium and concentration of the strontium in metastatic lesions. Increased whole-body retentions are due to the avid uptake of strontium in lesion sites, and in some cases decreased renal plasma clearance may also contribute to this effect. The whole-body retention, as measured by urinary excretion of strontium, correlated positively with the extent of disease. Plasma-strontium concentrations were lower than expected, indicating that the strontium was being rapidly taken up in the metastases.

We have shown that ^{85}Sr, and therefore ^{89}Sr, is readily localized in metastatic lesions. Additionally, strontium is strongly retained in these sites, and, as a result, can deliver a radiation dose (median value: 68 cGy/MBq) that is thought to be sufficiently large to produce a therapeutic effect. These results are consistent with previously published values. Absorbed doses to red marrow were generally less by at least a factor of about 2 to 50. The degree of strontium concentration in the lesion sites, and the rate of washout from the lesion sites, appears to be independent of strontium whole-body kinetics. In patients with lower plasma clearance rates, strontium has more time to become absorbed in metastases; however, it is the metabolic activity of the lesion itself that determines the degree of strontium retention, and hence, the absorbed dose delivered to the metastases.

There remain several questions about strontium therapy that have yet to be answered. Chief among these is the manner in which the absorbed dose is transported through inhomogeneous material that makes up a metastatic lesion. Second, the pattern of strontium uptake within a metastasis must be known before an accurate measurement of dose can be made.

ACKNOWLEDGMENTS

Financial support for this work was provided by Amersham International. The authors wish to thank Dr. T.D. Cradduck for many helpful discussions and the technologists in the Department of Nuclear Medicine at Victoria Hospital for their work.

REFERENCES

1. Pecher C. Biological investigations with radioactive calcium and strontium: preliminary report on the use of radioactive strontium in the treatment of bone cancer. *Univ Calif Publ Pharmacology* 1942;11:117–149.
2. Lawrence JH, Wassermann LR. Multiple myeloma: a study of 24 patients treated with radioactive isotopes (^{32}P and ^{89}Sr). *Ann Intern Med* 1950;33:41–55.
3. Aziz H, Choi K, Sohn C, Yaes R, Rotman M. Comparison of P-32 and SHBI for bony metastases. *Am J Clin Oncol* 1986;9:264–268.
4. Tennvall J, Darte L, Lindgren R, El Hassan AM. Palliation of multiple bony metastases from prostatic carcinoma with strontium-89. *Acta Oncol* 1988;27:365–369.
5. Robinson RG, Spencer JA, Preston DF, Wegst AV, Martin NL. Treatment of metastatic bone pain with strontium-89. *Nucl Med Biol* 1987;14:219–222.
6. Kloiber R, Molnar CP, Barnes M. Sr-89 therapy for metastatic bone disease: scintigraphic and radiographic follow-up. *Radiology* 1987;163:719–723.
7. Robinson RG, Spicer JA, Blake GM, et al. Strontium-89: treatment results and kinetics in patients with painful metastatic prostate and breast cancer in bone. *Radiographics* 1989;9:271–281.
8. Firusian N, Mellin P, Schmidt CG. Results in strontium-89 therapy in patients with carcinoma of the prostate and incurable pain from metastases: a preliminary report. *J Urol* 1976;116:764–768.
9. Silberstein EB, Williams C. Strontium-89 therapy for the pain of osseous metastases. *J Nucl Med* 1985;26:345–348.
10. Blake GM, Zivanovic MA, McEwan AJ, Ackery DM. Sr-89 therapy: strontium kinetics in disseminated carcinoma of the prostate. *Eur J Nucl Med* 1986;12:447–454.
11. Blake GM, Zivanovic MA, Gray JM. Strontium kinetics in metastasised prostatic carcinoma: a comparison with the predictions of impulse response function analysis. *Nucl Med Commun* 1987;8:909–919.
12. Blake GM, Zivanovic MA, McEwan AJ, et al. Strontium-89 therapy: strontium kinetics and dosimetry in two patients treated for metastasising osteosarcoma. *Br J Radiol* 1987;60:253–259.
13. Blake GM, Zivanovic MA, Blaquiere RM, Fine DR, McEwan AJ, Ackery DM. Strontium-89 therapy: Measurement of absorbed dose to skeletal metastases. *J Nucl Med* 1988;29:549–557.
14. Loevinger R, Berman M. A revised scheme for calculating the absorbed dose from biologically distributed radionuclides. *MIRD pamphlet No. 1, revised.* New York: The Society of Nuclear Medicine; 1976.
15. Marshall JH, Lloyd EL, Runda JA, et al. Alkaline earth metabolism in adult man. *Health Phys* 1963;24:125–221.
16. Fleming JS. A technique for the absolute measurement of activity using a gamma camera and computer. *Phys Med Biol* 1979;24:176–180.
17. Macey DJ, Marshall R. Absolute quantitation of radiotracer in lungs using a gamma camera. *J Nucl Med* 1982;23:731–735.
18. Jones JP, Brill AB, Johnston RE. The validity of an equivalent point source (EPS) assumption used in quantitative scanning. *Phys Med Biol* 1975;20:455–464.
19. International Commission on Radiological Protection. Dosimetric model for bone. *ICRP publication 30: limits for intakes of radionuclides by workers. Part 1.* 1979:35–46.
20. Bevington PR. *Data reduction and error analysis for the physical sciences.* New York: McGraw-Hill; 1969:56–65.
21. Battermann JJ, Boon TA, van Es C, Moonen L, de Voogt HJ. Brachytherapy in the management of prostate cancer. In: Mould RF, ed. *Brachytherapy 2: proceedings of the fifth international SELECTRON users meeting.* The Hague: Nucletron International B.V.; 1989:159–164.
22. Kirk J, Gray WM, Watson ER. Cumulative radiation effect, part III. Short-lived sources. *Clin Radiol* 1973;24:1–11.
23. Mauch PM. Treatment of metastatic cancer to bone. In: Hellman S, Rosenberg SA, eds. *Cancer: principles and practice of oncology.* Philadelphia: L.B. Lippincott; 1982:1564–1568.
24. Cowan RJ, Chilton HM, Cooper MR, Ferree CR, Watson EE, Robinson RG. Hematological depression following therapy with strontium-89 chloride. *Clin Nucl Med* 1986;11:485–486.